

## EVIDENCE FOR RAPID ROTATION OF THE CARBON STAR V HYDRAE

CECILIA BARNBAUM

National Radio Astronomy Observatory,<sup>1</sup> 520 Edgemont Road, Charlottesville, VA 22903

MARK MORRIS

Department of Astronomy, University of California, Los Angeles, CA 90024

AND

CLAUDINE KAHANE

Observatoire de Grenoble, UJF, CERMO, B.P. 68, F-38402 St. Martin d'Hères Cedex, France

Received 1994 November 8; accepted 1995 March 23

### ABSTRACT

The carbon star V Hya is known to have a bipolar circumstellar outflow and an unusual photospheric spectrum. After measuring the changes in the photospheric velocity and carrying out a spectral broadening analysis over 10 photometric phases, we conclude that rotation due to spin-up by a companion in a common envelope configuration is the most compelling explanation for all the data taken together. After considering the spectral and velocity behavior of 74 other carbon stars, we find that V Hya is alone in our sample in having such obvious phase-dependent broadening.

In this paper we detail the broadening results and explore other possible causes of spectral broadening in late-type stars. In particular, we find that: (1) the spectral broadening in V Hya varies about a mean value of  $13.5 \text{ km s}^{-1}$  (with total variation of  $9 \text{ km s}^{-1}$ ) in concert with the photometric phase and with a phase relationship consistent with that expected for a rapidly rotating star that conserves angular momentum as it pulsates, (2) V Hya's unusual, very long secondary period of 6500 days might be attributed to a coupling of radial pulsation (529 day period) with rotation, (3) the upper limit on the ultraviolet continuum flux favors a common envelope versus detached binary system, (4) the variability type, Mira versus semiregular variable, is uncertain since V Hya demonstrates spectral characteristics of both, and (5) the evolutionary placement on the asymptotic giant branch is in question since V Hya appears to lack  $^{99}\text{Tc}$ , a signature element of third dredge-up whose absence suggests that a mass transfer event in the past might be responsible for V Hya's carbon and s-process element enhancement.

*Subject headings:* stars: AGB and post-AGB — stars: carbon — stars: individual (V Hydrae) — stars: rotation

### 1. INTRODUCTION

Stars on the asymptotic giant branch (AGB) shed their outer layers, surrounding themselves with cool, dusty circumstellar envelopes. Carbon stars on the AGB, for example, typically lose mass at  $\geq 10^{-7} M_{\odot} \text{ yr}^{-1}$  (Claussen et al. 1987). The resulting circumstellar outflows have been mapped in CO ( $J = 1-0$  and  $J = 2-1$ ) for a number of AGB stars, and most demonstrate spherical geometry. Since bipolar outflows are apparently rare among AGB stars, it is surprising that a large fraction ( $>50\%$ ) of planetary nebulae are aspherical (Zuckerman & Aller 1986). How bipolar outflows develop around evolved stars is not understood, but several models have been proposed. Some of these models invoke rotation of the central star (Mufson & Liszt 1975; Phillips & Reay 1977; Pascoli 1987). Other models invoke binarity as a means to collimate mass loss (Morris 1987, 1990; Soker & Livio 1989; Soker 1992, 1993); Iben & Livio (1993) have reviewed the role of common envelope binaries in the formation of aspherical planetary nebulae.

The carbon star V Hya has a distinctly bipolar circumstellar envelope, as observed in CO ( $J = 1-0$ ) (Tsuiji et al. 1988; Kahane, Maizels, & Jura 1988). Low-resolution optical spectra of the blue region show bright atomic emission lines blue-

shifted by  $155 \text{ km s}^{-1}$  from the rest velocity of V Hya (Lloyd Evans 1991), and the  $4.6 \mu\text{m}$  absorption line of the fundamental CO rotation-vibration band is blueshifted by  $120 \text{ km s}^{-1}$  from rest (Sahai & Wannier 1988). The blueshifted material likely arises in a high-velocity lobe of the bipolar jet from an accretion disk in a binary system (Sahai & Wannier 1988; Lloyd Evans 1991). Our high-resolution optical spectra suggest that V Hya is rotating (Kahane et al. 1988, 1993). Inasmuch as a binary companion would be required to account for the amount of angular momentum implied for the atmosphere of V Hya, we can attempt to link these facts and to formulate a coherent picture of asymmetric mass loss, binarity, rotation, and common envelope evolution. In Kahane et al. (1993) we presented a preliminary discussion of our  $^{12}\text{CO}$  radio map ( $J = 2-1$ ) of V Hya, as well as a preliminary model of the outflow. Here, we present the optical data which provide evidence that V Hya is rotating, and we argue that it is this rotation that induces the asymmetric mass loss. In a separate paper, the CO mapping data and modeling of the bipolar outflow will be described in detail (Kahane et al. 1995).

Not only is V Hya apparently rotating, but it also has the pulsational properties of a long-period variable. Indeed, the atmospheric motions owed to rotation and pulsation might be comparable in this system, in which case the coupling between these motions is considerable, leading to a time-varying rotation rate, to coherent, large-scale atmospheric circulation patterns, and perhaps to resonant interactions between the two

<sup>1</sup> Operated by Associated Universities, Inc., under cooperative agreement with the National Science Foundation.

motions. In addition, the measurable manifestations associated with these phenomena can help one to identify the mode of pulsation.

In this paper we present a set of high-resolution, optical spectroscopic observations extending over 6 yr. The observational techniques are described in § 2, while the methodology and results are presented in §§ 3 and 4, respectively. There, we present our finding that the atmospheric radial velocity and the line width both vary periodically with the photometric phase of the star. In § 5, the discussion, we point out that the relationship between the velocities and their phase is that expected for a rotating star in which the dominant pulsational mode is the fundamental, perturbed as it may be by the presence of rotation. Finally, in § 6 we conclude by pointing out that V Hya may serve as a key object for understanding the brief, but important, common envelope phase of stellar evolution.

## 2. OBSERVATIONS

All observations were obtained with the 120 inch (3 m) Shane Telescope, coudé focus, at Lick Observatory. We first observed V Hya in 1987 May, when the star was at maximum light. For that observation and the one in 1988 March, we used the 900 line  $\text{mm}^{-1}$  grating in second order, producing a linear reciprocal dispersion of  $4.9 \text{ \AA mm}^{-1}$  with spectral resolution of  $0.18 \text{ \AA}$  for a total of  $56 \text{ \AA}$  centered at  $7460 \text{ \AA}$ . For these two observations with a conventional spectrograph, we used an image slicer built by S. Vogt of the University of California, Santa Cruz. The 10 observations of V Hya from 1988 May through 1993 January were taken with the Hamilton echelle spectrograph, which produces high-resolution spectra ( $0.13 \text{ \AA}$  at  $6100 \text{ \AA}$ ) with a linear reciprocal dispersion ranging from  $2.8 \text{ \AA mm}^{-1}$  in the blue to  $4.3 \text{ \AA mm}^{-1}$  in the red with broad wavelength coverage, from  $5085$  to  $7850 \text{ \AA}$  (see Vogt 1987 for a description of the equipment). The detector used with both spectrographs was a TI  $800 \times 800$  CCD. A journal of the observations appears in Table 1 and includes the photometric phase of V Hya at each observation. The light curve was derived by fitting to photometric data provided by AAVSO (Mattei 1990).

The data were reduced with the IRAF software package. The bias was subtracted from the image, and a quartz lamp

TABLE 1  
JOURNAL OF THE OBSERVATIONS OF V HYA

Spectrograph <sup>a</sup>	UT Date	JD	
		+ 2,400,000	$\phi^b$
Conventional grating .....	1987 May 18	46,933.77	0.06
Conventional grating .....	1988 Mar 1	47,222.88	0.61
Echelle grating .....	1988 May 31	47,312.67	0.78
Echelle grating .....	1988 Dec 29	47,524.98	0.18
Echelle grating .....	1989 May 15	47,661.70	0.44
Echelle grating .....	1989 Dec 10	47,871.01	0.83
Echelle grating .....	1990 Mar 10	47,960.76	0.00
Echelle grating .....	1990 Jun 7	48,049.69	0.17
Echelle grating .....	1990 Nov 27	48,223.02	0.50
Echelle grating .....	1990 Dec 9	48,234.98	0.52
Echelle grating .....	1992 Dec 4	48,961.00	0.89
Echelle grating .....	1993 Jan 2	48,990.05	0.94

<sup>a</sup> Conventional grating is  $900 \text{ line mm}^{-1}$  in second order with  $56 \text{ \AA}$  centered at  $7460 \text{ \AA}$ , and the echelle grating is the Hamilton echelle, producing 40 spectral orders, from  $5080$  to  $7850 \text{ \AA}$ .

<sup>b</sup> The phase,  $\phi$ , is the light phase, conventionally defined to be  $\phi = 0.0$  at maximum light and  $\phi = 0.45$  at minimum light.

provided the flat field. In all cases, Th-Ar spectra were used for wavelength calibration. Echelle reduction procedures are discussed by Goodrich & Veilleux (1988), and specifics of the reduction method we used for these data are presented in Barnbaum (1992a).

## 3. METHODS

### 3.1. Characteristics of Carbon Star Spectra

Optical spectra of carbon stars are characterized by a set of very closely spaced molecular absorption lines, namely, the vibration-rotation transitions of CN and  $\text{C}_2$  (see Fig. 1). The continuum is entirely obscured throughout the optical region, and atomic absorption lines are so overwhelmed by the molecular transitions that only the Doppler cores of strong atomic lines are distinguishable. Since the wings of even the strongest atomic lines are not visible and the placement of the continuum is unknown, direct measurements of equivalent width are not possible without performing spectral synthesis using model atmospheres and all the assumptions entailed. However, although complicated in appearance, high-resolution optical spectra of different carbon stars are very similar (see Barnbaum 1994). Line ratios sometimes vary significantly from star to star, but nearly every absorption dip is reproduced in the spectrum of every star. This close similarity allows detailed comparisons among spectra in spite of the absence of a continuum.

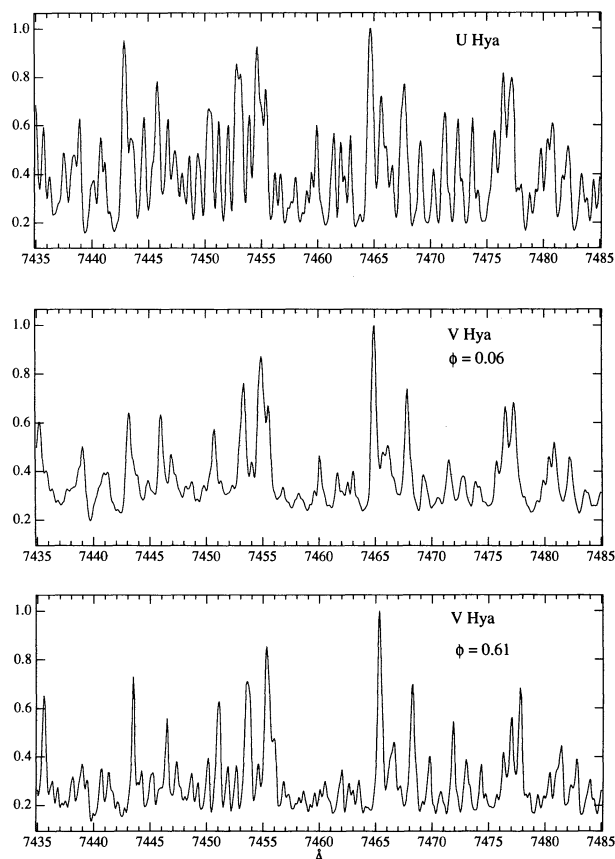


FIG. 1.—Spectra of the carbon stars, U Hya and V Hya. The light phase,  $\phi$ , is defined to be 0 at photometric maximum (where 0.5 is at minimum for a symmetric light curve). The spectra are corrected for heliocentric motion; any wavelength offset of absorption features from rest is due to the velocity of the star.

In this study, we exploit the strong similarity of the spectra to investigate the line broadening in V Hya.

### 3.2. Radial Velocity Measurements

Cross-correlation yields accurate radial velocities relative to the template spectrum used (see Tonry & Davis 1979). The radial velocity of V Hya was measured by cross-correlating 25–30 spectral orders of each observation with those of a template. The template used for each observation of each star and all the atomic line velocities are presented in Barnbaum (1992a). The great number of molecular lines in carbon star spectra ensure accurate velocity measurements with respect to the template. This technique uses all the information in a spectrum and therefore represents a statistical average of the motion of the atmospheric layers giving rise to the CN absorption lines (Barnbaum 1992a). In addition, we have measured the velocities of a few relatively strong atomic lines by fitting a parabola to the line core; these lines include Mg  $\text{I}$   $\lambda$ 5183.60 and the resonance lines of K  $\text{I}$   $\lambda$ 7896.98 and Li  $\text{I}$   $\lambda$ 6707.84. It has been shown that the velocity differences among strong atomic absorption lines, as well as their amplitude of variation with phase, are significantly greater for Miras than for semi-regular (SR) variables (Barnbaum 1992a). We discuss the absorption line velocities of V Hya in § 5.1.2.

### 3.3. Rotational Broadening Analysis

Line widths in the spectra of cool stars are affected by special properties of their extended atmospheres. If the atmosphere has strong velocity gradients, for example, then the resulting weak line doubling might cause some apparent smearing of the optical spectrum. However, broadening of a single absorption line can be caused by rotation, by macroturbulence, or by an increase in opacity. The very subtle differences among these broadening mechanisms are manifest in the wings of the line, and these effects are difficult to distinguish even in the ideal circumstance when the continuum is present and the line unblended (Gray 1976). Given the special problems with carbon star spectra, i.e., no visible continuum and heavily blended lines, a distinction between macroturbulence and rotation cannot be made with certainty. We assume in this analysis that the broadening is due to rotation, though other possibilities are discussed in § 5.2.

Of the methods used to measure rotational broadening, those that require a clean line profile (e.g., Carroll 1933) cannot be used for the optical spectra of carbon stars. Cross-correlation techniques are more promising in this case. For example, Soderblom, Pendelton, & Pallavicini (1989) established F and G dwarf rotation velocity standards by cross-correlating the spectrum of a target star with a template made by convolving a synthetic spectrum with assumed rotation profiles. For the vastly more complicated carbon star spectra, we employ a variation of this technique by using the spectra of program stars as templates, thereby exploiting their strong similarity. This method gives *relative* rotation velocities.

Our method compares artificially broadened stellar templates with the spectra of V Hya and finds the rotation velocity corresponding to the best fit. To obviate the need to know the location of the continuum, the area under each spectrum of a given order was first normalized to unity. Each template was broadened by convolution with a rotation profile, as described in Gray (1976), sequentially from  $v \sin i = 1$  to  $25 \text{ km s}^{-1}$ , where  $v$  is the equatorial velocity and  $i$  is the inclination angle of the star to the line of sight. These artificially broadened

templates were then compared both visually and by a point-by-point least-squares fit to aligned spectra of V Hya. That is, each artificially broadened template ( $T$ ) is aligned in wavelength with the corresponding spectrum of V Hya ( $S$ ) by minimizing the sum

$$\sum_i^N \sqrt{(T_i - S_i)^2}, \quad (1)$$

where  $i$  is summed over all points in the spectrum, typically  $N = 790$ . The  $v \sin i$  of the artificially broadened template having the smallest minimized value of expression (1) is considered the best fit. If the spectrum of the template ( $T$ ) is inherently broader than that of the program star ( $S$ ), expression (1) is smallest when the artificial template is unbroadened. The rotation velocity difference between two stars compared in this manner is the quadrature of the difference. The rotation velocity of an AGB star with a radius of  $\sim 400 R_{\odot}$ , evolving in isolation, is not likely to be greater than  $2 \text{ km s}^{-1}$  even if its main-sequence progenitor rotated at breakup velocity. Therefore, when the velocity is measured relative to a narrow-line star and when it is  $\geq 2 \text{ km s}^{-1}$ , it can be taken as the full measure of broadening. Given the lack of any line wings in the optical spectra of carbon stars, the only method that would be better than the one described here would be spectral synthesis using sophisticated model atmospheres which are not currently available.

For the echelle observations, approximately 20 spectral orders of each observation, from 6000 to 7800 Å, were selected for the broadening analysis after eliminating orders dominated by telluric features or by very strong, variable atomic lines (such as Na D or having low signal-to-noise ratio). The remaining orders were averaged to get a mean  $v \sin i$ . The dispersion of values from order to order, typically  $\sim 3 \text{ km s}^{-1}$ , provides an estimate of the uncertainty of this method.

As a check of our basic method, we observed two of the F6 V standard rotation stars measured by Soderblom et al. (1989). The slower rotator  $\gamma$  Ser is with  $v \sin i = 9.3 \text{ km s}^{-1}$ , and so we have broadened it artificially to fit HD 113022, which has  $v \sin i = 21.5 \text{ km s}^{-1}$ . Since velocities measured in this way add in quadrature, we expect that the difference of the squares of the true rotation velocities should equal the square of the best-fit rotation velocity of template  $\gamma$  Ser to HD 113022; that is, we expect a fit rotation velocity of  $19.4 \text{ km s}^{-1}$ . We measure the best-fit rotation velocity to be  $20.8 \text{ km s}^{-1}$ , with a standard deviation from order to order of  $0.9 \text{ km s}^{-1}$ , which we deem to be a satisfactory result.

The brute force convolution of the entire spectrum by a rotational broadening profile misrepresents, to some extent, the shape of the narrow quasi-continuum windows between absorption lines. The ideal procedure would be to locate and broaden each and every absorption line, but the density of lines makes this impracticable until spectral synthesis using realistic model atmospheres of carbon stars becomes available. However, the fraction of the spectrum which is between lines is small enough that we do not feel that our procedure leads to any serious misrepresentation of the broadening.

## 4. RESULTS

### 4.1. Velocity Characteristics of V Hya: General Results

#### 4.1.1. Comparison Stars

We have compared 74 template carbon star spectra with V Hya; 142 separate comparisons were made over nine observ-

TABLE 2  
PROPERTIES OF TEMPLATE STARS COMPARED TO V HYA

Star	Spectral Type		Variability	Period (days)	Star	Spectral Type		Variability	Period (days)
V Hya	N6	C6,3e	M/SR	529.2	ZZ Gem	Ne	C5,3e	M	317
AQ And	N	C5,4	SR	...	CZ Hya	Ne	Ce	M	442
EU And	R	C4,4J	SR	140–175 <sup>a</sup>	RY Hya	N	C6,4e	SRb	529
SU And	N	C6,4	Lc	...	U Hya	N2	C6,5	SRb	450
VX And	N7	C4,5J	SRa	369	Y Hya	N3p	C5,4	SRb	302.8
V Aql	N6	C6,4	SRb	353	R Lep	N6e	C7,6e	M	427.1
V374 Aql	Ne	C7,3e	SRa	456.5	HK Lyr	N4	C6,4	Lb	...
AZ Aur	N0e	C7,1e	M	415.9	T Lyr	R6	C6,5J	Lb	...
EL Aur	N3	C5,4	Lb	...	U Lyr	N0e	C4,5e	M	455.6
FU Aur	N0	C7,2	Lb	...	CL Mon	N6e	C6,3e	M	497.2
S Aur	N3	C4,4	SR	590.1	CZ Mon	N5	C4,5	Lb	...
TX Aur	N3	C5,4	Lb	...	DF Mon	N	C4,4	Lb	...
UU Aur	N3	C5,3	SRb	234	GY Mon	N3R8	C6,3	Lb	...
UV Aur	Ne	C6,2epJ	M	394.4	TW Oph	N	C5,5	SRb	185
S Cam	R8e	C7,3e	SRa	327.3	V Oph	N3e	C5,2e	M	298
ST Cam	N5	C5,4	SRb	300	BL Ori	N	C6,3	Lb	...
U Cam	N5	C3,9e	SRb	...	GK Ori	N	C4,4	SR	236
UV Cam	R8	C5,3J	SRb	294	RT Ori	N	C6,4	SRb	321
HV Cas	Ne	C4,3e	M	527	W Ori	N5	C5,4	SRb	212
W Cas	...	C7,1e	M	405.6	RZ Peg	CSe	C9,1e	M	439.4
X Cas	N1e	C5,4e	M	422.8	SY Per	N3e	C6,4e	SRa	474
S Cep	N8e	C7,4e	M	487	TX Psc	N0	C7,2	Lb	...
W CMa	N	C6,3	Lb	...	Z Psc	N0	C7,2	SRb	144
R CMi	CSep	C7,1eJ	M	337.8	AC Pup	N	C5,4	Lb	...
T Cnc	N6R6	C3,8	SRb	482.3	R Scl	Np	C6,5e	SRb	370
X Cnc	N3	C5,4	SRb	195	SU Sco	N0	C5,5	SR	414
V CrB	N2e	C6,2e	M	358	S Sct	N3	C6,4	SRb	148
Y CVn	N3	C5,4J	SRb	157	SS Sgr	N/R3	C3,4	SRb	...
RS Cyg	N0ep	C8,2e	SRa	417.4	SZ Sgr	N	C7,3	SRb	73
TT Cyg	N3e	C5,4e	SRb	118	V2548 Sgr	N3	...	SRa	159
V778 Cyg	N	C4,5J	Lb	302 <sup>a</sup>	V781 Sgr	N0	C	Lb	...
RY Dra	N4p	C4,5J	SRb	172.5	TT Tau	N3	C4,2	SRb	166.5
T Dra	N0e	C6,2e	M	421.2	TU Tau	N3	C5,4	SRb	190
UX Dra	N0	C7,3	SRa	168	Y Tau	N2e	C6,5e	SRb	241.5
BM Gem	N	C5,4J	SRb	...	TMSS-30293	...	...	...	...
TU Gem	N3	C6,4	SRb	230	VY UMa	N0	C6,3	Lb	...
VX Gem	Nep	C7,2e	M	379.4	RU Vir	R3ep	C8,1e	M	436.2
					SS Vir	Ne	C6,3e	M	354.7

<sup>a</sup> The periods for EU And and V778 Cyg are taken from Little-Marenin, Benson, & Cadmus 1993.

ing runs, and 132 of these use  $\sim 20$  spectral orders each. We find that 73 of the 74 template spectra must be broadened by some amount (at all observed photometric phases of V Hya) for a best fit to V Hya. The only exception is S Aur, which needs no broadening to fit V Hya when both are at minimum light. Two other stars, SS Vir and S Cep, have comparatively broader spectral lines than most other carbon stars. S Cep shows weak line doubling that might contribute to the smeared appearance of the spectrum (see § 5.2, but this is not the case in S Aur or SS Vir, and these stars are discussed below in § 4.3. Table 2 lists all the template stars, their spectral classification, variability type, and period.

One template star, U Hya, was observed concurrently with V Hya for all but one of the observations. Figure 1 displays sample spectra of V Hya near both minimum and maximum light and of template U Hya. The rotational broadening fits to V Hya using U Hya and one other template star (for the one observation when spectra of U Hya were not obtained) are presented in Table 3 and plotted in Figure 2. U Hya was chosen for its frequency of observation and relative stability in radial velocity. To check the stability of its line width, we compared spectra of U Hya taken at different phases and found that there are no broadening changes; that is, the best fit of one spectrum of U Hya as template to another is that which

has no artificial broadening. Since the limit of the sensitivity of this technique is less than  $2 \text{ km s}^{-1}$  rotation velocity, we consider this to be the uncertainty in the variation of the template star. Figure 2 (*top*) displays the radial velocity (*right-hand axis*) and the rotation velocity (*left-hand axis*) for V Hya versus Julian Day, plotted on top of the photometric light curve provided by the AAVSO (Mattei 1990). The scale of the variation is  $\sim 3.5$  visual magnitudes. Rotation velocity and radial velocity folded with phase appear in Figure 2 (*bottom*).

#### 4.1.2. Radial Velocity

The full range of the radial velocity variation is  $10.7 \text{ km s}^{-1}$ , and the phase of that variation is offset from the photometric phase,  $\phi$  (where  $\phi = 0$  refers to maximum light; V Hya displays a typically skewed light curve and reaches minimum light between  $\phi = 0.4$  and  $0.5$ ) (see Fig. 2). To a first approximation, an AGB star achieves smallest radius near maximum light and largest radius near minimum light, owing predominantly to a change in photospheric temperature with stellar radius. A lag in the radial velocity from photometric maximum is therefore expected if the velocity changes are due to radial pulsation. While the phases of the radial velocity extrema are not very well determined, there does appear to be a lag of about a tenth of a period between the light and the velocity extrema. That

TABLE 3  
ROTATIONAL BROADENING FIT TO V HYA

Template	$\phi$ of Template <sup>a</sup>	UT Date	Rotation Velocity $v \sin i$ Fit to V Hya ( $\pm 2 \text{ km s}^{-1}$ ) ( $\text{km s}^{-1}$ )	Radial Velocity of V Hya <sup>b</sup> ( $\pm 1.5 \text{ km s}^{-1}$ ) ( $\text{km s}^{-1}$ )	$\phi$ of V Hya <sup>a</sup>
U Hya .....	0.38	1987 May 18	16.0	-6.6	0.06
S Sct.....	...	1988 Mar 1	10.0	2.4	0.61
U Hya .....	0.23	1988 May 31	11.5	-0.3	0.78
U Hya .....	0.70	1988 Dec 29	12.3	-6.1	0.18
U Hya .....	0.00	1989 May 15	10.6	0.9	0.44
U Hya .....	0.47	1989 Dec 10	12.5	2.9	0.83
U Hya .....	0.67	1990 Mar 10	15.6	-6.9	0.00
U Hya .....	0.86	1990 Jun 7	11.0	-5.2	0.17
U Hya .....	0.25	1990 Nov 27	6.6	3.4	0.50
U Hya .....	0.28	1990 Dec 9	6.8	2.9	0.52
U Hya .....	0.89	1992 Dec 4	16.0	-4.4	0.89
U Hya <sup>c</sup> .....	0.89	1993 Jan 2	16.7	-7.3	0.94

<sup>a</sup> The phase,  $\phi$ , indicates maximum light at  $\phi = 0.0$  and minimum light at  $\phi = 0.45$ .

<sup>b</sup> All radial velocities were cross-correlated with a template, and the data are presented in detail in Barnbaum 1992a.

<sup>c</sup> U Hya observed on 1992 Dec 4 was used for comparison with V Hya observed on 1993 Jan 2.

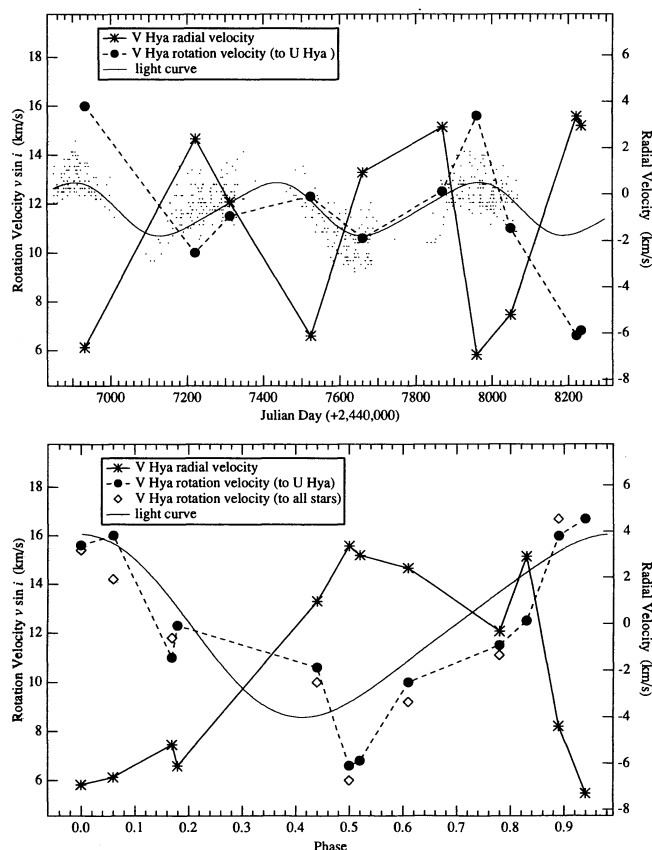


FIG. 2.—*Top*: Rotation velocity,  $v \sin i$ , and radial velocity of V Hya vs. Julian Day. The rotation velocity axis is on the left, and the radial velocity axis is on the right. The rotation velocity plotted is the result of a comparison with the SR variable template U Hya, and we estimate the error to be  $2 \text{ km s}^{-1}$ . The radial velocities are from cross-correlation analysis and are presented in full in Barnbaum (1992a). The radial velocity error is  $\pm 1.5 \text{ km s}^{-1}$ . The visual light curve (solid curve) was fitted to data provided by the AAVSO (points) (Mattei 1990). Note in this plot that the maximum photometric amplitude corresponds to maximum light and the scale of the variation, not shown in the plot is  $\sim 3.5$  visual magnitudes going from  $9.5 m_v$  to  $6 m_v$ . *Bottom*: Rotation and radial velocities plotted vs. the light phase of V Hya. The  $v \sin i$  fit averaged from all stars also appears, as well as the light curve fitted to the AAVSO data.

this is somewhat less than the 0.25 of a period expected in the idealized case can be ascribed to a combination of the variation of the depth of the visual photosphere during the light cycle (e.g., Hinkle & Barnes 1979) and a lag between the visual and bolometric magnitudes resulting from phase-dependent dust formation.

#### 4.1.3. Rotation Velocity

The apparent rotation velocity,  $v \sin i$ , measured with respect to U Hya, averages  $\sim 11 \text{ km s}^{-1}$  and undergoes a total periodic variation of  $\sim 9 \text{ km s}^{-1}$ . If the star is rotating, then by conservation of angular momentum, the largest rotation velocity is expected near maximum light and the smallest near minimum light. The fitted values of  $v \sin i$  versus photometric phase (see Fig. 2, *bottom*) demonstrate that the line-broadening behavior is roughly consistent with this, although the minimum rotational velocity might occur  $0.1 \pm 0.1$  of a period after minimum light.

Along with the rotation fits using the template U Hya, the mean  $v \sin i$  with respect to all concurrently observed templates at a given phase of V Hya is also plotted in Figure 2 (*bottom*), and the agreement is very good. To give an example of the variation of  $v \sin i$  among spectral orders for a given observation and the range of values among template stars, Tables 4 and 5 present templates with their phase and the  $v \sin i$  fit per order to V Hya at its photometric minimum (Table 4) and maximum (Table 5). The standard deviation of the mean for each observation is indicated at the bottom of each table and is fairly consistent. The absolute rotation velocity of V Hya is uncertain, but the *relative* variation in broadening from minimum to maximum light changes by  $\sim 9 \text{ km s}^{-1}$ .

#### 4.2. Line-Broadening Fits to V Hya by Variable $\Gamma$ type

V Hya and the template stars used for comparison are long-period variables (LPV) and are categorized as either Mira, SR, or Lb (irregular) variables. These three types of variables are so classified by their (1) amplitude of visual light change and (2) regularity of period (Kholopov 1985). It has been known for some time that, on average, Miras have longer and more regular periods, deeper amplitudes of pulsation, and higher mass-loss rates than the SR or Lb variables (see Jura & Klein-

TABLE 4  
 TEMPLATE ROTATION VELOCITIES FIT TO V HYA AT  $\phi = 0.5$

Order <sup>a</sup>	TT Tau	TU Tau	TX Psc	U Hya	W Ori	RU Vir <sup>b</sup>	X Cnc	SS Vir <sup>b</sup>	EL Aur	TX Aur	S Cam
$\phi$ .....	...	...	...	0.25	...	0.09	0.54	0.98	...	...	0.89
19 .....	...	4	2	2	4	10	2	...	4	5	...
20 .....	3	5	2	6	5	6	6	7	6	6	5
21 .....	2	5	2	6	5	8	5	5	5	5	2
22 .....	5	7	5	7	7	11	8	12	7	7	6
23 .....	3	3	2	6	5	12	5	5	6	5	3
24 .....	6	6	3	7	7	9	7	8	6	6	5
25 .....	7	4	7	8	7	6	7	9	10	7	5
27 .....	2	2	2	5	2	12	3	3	4	3	2
28 .....	7	11	6	8	8	...	10	7	5	8	7
29 .....	3	10	2	6	6	2	7	2	9	8	7
32 .....	2	5	2	7	4	10	6	10	7	6	2
33 .....	7	9	7	8	9	3	8	6	10	10	5
35 .....	9	12	8	10	10	7	11	7	12	11	7
36 .....	5	8	3	8	7	...	8	12	9	8	8
37 .....	6	7	3	8	7	13	8	7	8	6	5
39 .....	2	5	2	3	2	2	2	5	5	5	2
40 .....	2	5	2	5	5	5	4	7	6	6	2
Average .....	4.4	6.4	3.5	6.5	5.9	7.8	6.3	7.0	7.0	6.5	4.6
$\sigma$ .....	2.3	2.8	2.2	2.0	2.2	3.7	2.6	2.8	2.3	2.0	2.1

<sup>a</sup> Spectral order number with 19 starting at  $\lambda = 6065 \text{ \AA}$  and 40 starting at  $\lambda = 7850 \text{ \AA}$ . Where ellipses occur, the S/N of the template spectrum was low.

mann 1992 and Kerschbaum & Hron 1992, for detailed discussion), and there is some evidence that Miras and SR variables of different period ranges might have different pulsational modes (Jura & Kleinmann 1992). It is reasonable, then, to suspect that the differences in pulsational behavior and in atmospheric velocity structure among the three types of variables might effect the line-broadening comparison to V Hya. For example, spectral broadening in Miras might be due, in part, to changes in temperature and opacity throughout a photometric period (discussed further in § 5.2) or to line doubling caused by a steep velocity gradient in the pulsating atmosphere.

We have compared the spectra of V Hya with those of 19 Mira, 16 Lb, and 38 SR variables. Table 6 separates the

average rotation velocity fits to V Hya according to the variability type of the templates; note that  $\phi = 0.17$  and  $0.18$  have been combined, as have  $\phi = 0.50$  and  $0.52$ . Figure 3 plots the rotation velocity fits by variability type of the template versus V Hya phase. It is clear from Figure 3 that Miras are intrinsically somewhat broader than the SR variables; that is, Miras consistently require a smaller  $v \sin i$  for a best fit to V Hya than do either SR or Lb variables. The spectra of some Miras obviously broaden and narrow over their photometric period, as shown, for example, in Figure 4 for the Mira CZ Hya. However, all the Miras in the sample at a variety of phases have narrower lines than V Hya (with the exception of S Aur, discussed in § 4.3). The line widths in Mira spectra may vary with phase due to line doubling, but there is no other evidence

TABLE 5  
 TEMPLATE ROTATION VELOCITIES FIT TO V HYA AT  $\phi = 0.0$

Order <sup>a</sup>	CZ Hya <sup>b</sup>	AC Pup	RY Hya	SS vir <sup>b</sup>	T Cnc	RU Vir <sup>b</sup>	VY Uma	W CMa	V CrB <sup>b</sup>	X Cnc	U Hya
$\phi$ .....	0.18	...	...	0.21	0.03	0.46	...	...	0.72	0.20	...
94 .....	12	12	14	13	16	...	12	11	14	15	12
93 .....	17	15	14	14	16	8	16	15	17	17	15
92 .....	14	15	13	12	15	6	15	13	15	16	15
91 .....	17	16	15	16	17	10	16	16	18	18	17
90 .....	16	16	13	16	16	12	16	15	15	17	16
89 .....	16	17	16	16	15	9	17	17	17	18	17
88 .....	18	17	19	14	13	17	18	16	19	17	18
86 .....	13	16	14	16	18	...	15	14	9	16	16
85 .....	15	18	15	21	18	2	16	16	15	19	16
84 .....	11	13	16	11	13	2	13	13	11	13	11
81 .....	16	15	11	15	15	11	15	14	17	15	16
80 .....	17	18	15	16	17	14	17	17	18	18	18
78 .....	20	19	17	20	20	12	2	20	18	21	22
77 .....	19	17	16	18	18	10	18	17	18	19	17
76 .....	15	16	14	14	15	3	16	16	11	17	16
74 .....	10	12	10	8	15	2	14	13	11	15	12
73 .....	12	11	8	9	14	5	11	11	14	13	9
Average .....	15.2	15.5	14.1	14.6	15.9	7.5	14.5	14.9	15.1	16.7	15.5
$\sigma$ .....	2.8	2.3	2.6	3.4	1.9	4.9	3.8	2.3	3.1	2.1	3.1

<sup>a</sup> Spectral order number, with 19 starting at  $\lambda = 6065 \text{ \AA}$  and 40 starting at  $\lambda = 7850 \text{ \AA}$ . Where ellipses occur, the S/N of the template spectrum was low.  
<sup>b</sup> Mira variable.

TABLE 6  
ROTATIONAL BROADENING FITS TO V Hya BY VARIABILITY TYPE:  
 $v \sin i$  (km s<sup>-1</sup>)

Phase of V Hya	Type of Entry	SR	Mira	Lb	All Stars
0.00	Mean	17.5	13.4	15.3	15.4
	$\sigma$	2.9	1.1	...	3.3
	No. of stars	8	8	3	19
0.06 <sup>a</sup>	Mean	15.5	9	...	14.2
	$\sigma$	2.6	...	...	3.7
	No. of stars	4	1	...	5
0.17 + 0.18	Mean	13.4	7.1	13.9	11.8
	$\sigma$	1.0	...	...	3.6
	No. of stars	6	3	2	11
0.44	Mean	10.8	7.7	11.2	10.0
	$\sigma$	2.9	2.4	...	3.0
	No. of stars	10	5	2	17
0.50 + 0.52	Mean	7.2	4.5	5.4	6.0
	$\sigma$	2.0	2.8	1.2	2.9
	No. of stars	13	5	8	26
0.61 <sup>a</sup>	Mean	10.3	5	...	9.2
	$\sigma$	3.4	...	...	3.7
	No. of stars	4	1	...	5
0.78	Mean	13.8	7.5	...	11.1
	$\sigma$	1.9	2.1	...	3.9
	No. of stars	9	6	...	15
0.83	Mean	12.5	12.1	12.7	12.5
	$\sigma$	2.7	2.6	1.2	2.4
	No. of stars	23	10	9	42
0.89	Mean	16.7	...	...	16.7
	$\sigma$	...	...	...	...
	No. of stars	2	...	...	2
0.94	Mean	16.7	...	...	...
	$\sigma$	...	...	...	...
	No. of stars	1	...	...	...

<sup>a</sup> Spectra from the conventional grating with one order centered at 7560 Å; all other entries are from the echelle spectrograph.

that the line-width variations are caused by rotation in these stars.

High-excitation absorption lines in the infrared (CO) arise lower in the atmosphere than optical lines and have been described to double near maximum light due to steep velocity gradients (see Hinkle, Hall, & Ridgway 1982). Then line doubling in the optical region might be expected to occur in stars with deep amplitudes of pulsation. Weak line doubling in the

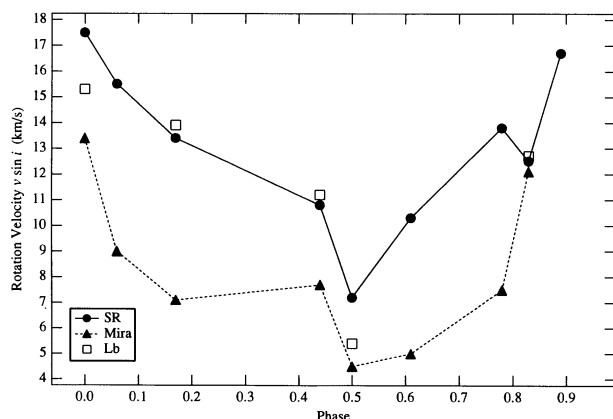


FIG. 3.—Average  $v \sin i$  of V Hya fitted by variability type of the templates used and plotted vs. the photometric phase of V Hya.

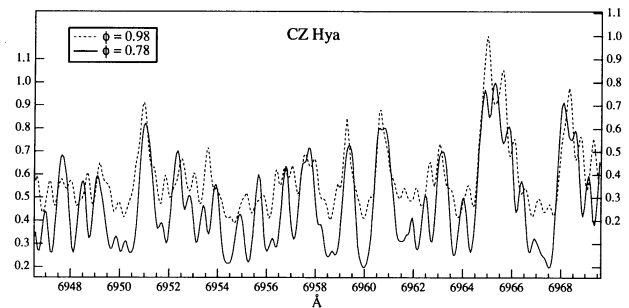


FIG. 4.—Example of intrinsic line broadening in a Mira carbon star CZ Hya at different photometric phases. The normalization is shown for the spectrum at  $\phi = 0.78$  and at  $\phi = 0.98$  on the left and right axes, respectively. The photometric phase was calculated from the epoch (JD 2,427,546) and period (442 days) given by Kholopov (1985) and may be inaccurate. The observations were separated by  $\sim 7$  months, being taken on 1989 May 16 and December 10. The peak of the cross-correlation function comparing CZ Hya with other carbon stars is double peaked; we attribute the spectral broadening to line doubling.

optical has been previously described in Mira carbon stars near maximum light (Phillips & Freedman 1969; Barnbaum 1992a). Such line splitting, although not demonstrated in all Miras of our sample, is clearly present in a few. For a subset of these, the cross-correlation function, which compares their spectra to a standard template to measure radial velocity, is double peaked or asymmetric. When present, this phenomenon is only seen with high resolution. An example of line doubling is shown in Figure 4 for CZ Hya just before maximum light. Despite the pronounced doubling in this and a few other stars (AZ Aur with 17 km s<sup>-1</sup>, ZZ Gem with 15 km s<sup>-1</sup>, and V Oph with 10 km s<sup>-1</sup> splitting; Barnbaum 1992a), their spectra still need to be broadened to fit V Hya. Furthermore, the spectra of V Hya over 12 observations are well distributed in phase and have shown neither doubled absorption lines nor an asymmetric peak in the cross-correlation function comparing V Hya to narrow-line templates.

If the doubling of absorption is subtle and just below the resolution of the spectrograph (2.5 km s<sup>-1</sup>), a slight broadening of the lines might be noticed rather than a clear splitting of single features. Thus, if the *template* spectra themselves are broadened by barely resolved doubling, then the fits of these templates to V Hya would give a lower  $v \sin i$  than would templates without line doubling. We suspect that this might contribute to the dependence of the rotation velocity fits on the variability type of the templates. However, since the spectrum of V Hya at its narrowest is still broader than that of other Miras at their broadest, we conclude that the dominant source of line broadening in V Hya is not owed to unresolved or strongly blended absorption line doubling.

The similarity of the average broadening curves of SR and Mira templates is striking (see Fig. 3). The mean difference in rotation velocity fits to V Hya between Mira and SR variables is 4.3 km s<sup>-1</sup>, and the change in rotation with phase is closely similar for all three variable types. The  $v \sin i$  fits for SR and Mira templates reach extrema of 17.5 and 13.5 km s<sup>-1</sup>, respectively, at maximum light. If V Hya is a true Mira, which remains unclear (see § 5.1), then some intrinsic line broadening might arise due to pulsation effects. In this case the rotation fits using the Mira templates (13.5 km s<sup>-1</sup> at maximum light) would be more appropriate as a relative measure of  $v \sin i$ . However, since the evolutionary status and variability type of V Hya are not certain, we regard this  $v \sin i$  as a lower bound.

#### 4.3. Two Other Carbon Stars with Significant Spectral Broadening: S Aur and SS Vir

There are two carbon stars in our sample (S Aur and SS Vir) that have comparatively broader spectral lines than most other carbon stars, but line doubling, if present, is not the obvious cause.

S Aur is a long period (590 day) SR variable with very weak H $\alpha$  emission. All radial velocity measurements of S Aur (at  $\phi = 0.46, 0.54,$  and  $0.95$ ) are strongly redshifted from center-of-mass motion (measured by circumstellar CO ( $J = 1-0$ ) by more than  $7 \text{ km s}^{-1}$ , as is typical of Miras (Barnbaum 1992b; Barnbaum & Hinkle 1995). However, these radial velocities do not vary by more than  $\sim 3 \text{ km s}^{-1}$  from minimum to maximum light. With only three observations, the variation is not well determined, but in V Hya, the greatest change in velocity occurs between  $\phi = 0.45$  and  $0.95$ , whereas the velocity of S Aur is stable over this same phase interval (velocities are listed in Barnbaum 1992a). The spectral broadening in S Aur, as compared with other templates, changes only from  $\sim 10$  to  $13 \text{ km s}^{-1}$  from minimum to maximum light. It is when S Aur is at maximum light and V Hya is at minimum light that S Aur is comparatively broader. No other star at maximum is as broad as V Hya at minimum light. Our limited phase coverage of S Aur and its uncertain current phase (the epoch was taken from Kholopov 1985) prevents a detailed investigation into the behavior of its optical spectrum. Its stability in radial velocity, however, merits further study.

SS Vir is a Mira variable with no obvious absorption line doubling, yet its spectra appear broadened. Compared with the template U Hya, SS Vir has a rotation velocity up to  $\sim 10 \text{ km s}^{-1}$  and only changes by  $\sim 2-3 \text{ km s}^{-1}$  from minimum to maximum light (over five observations at  $\phi = 0.21, 0.36, 0.38, 0.45,$  and  $0.98$ ). SS Vir were noted by Lambert et al. (1986) as having possibly doubled lines at  $2 \mu\text{m}$ . Like V Hya, SS Vir has a large variation in radial velocity,  $9 \text{ km s}^{-1}$  (Barnbaum 1992a). A most intriguing characteristic is that SS Vir has been found to lack the resonance line of  $^{99}\text{Tc}$  (Little, Little-Marenin, & Bauer 1987), a short-lived  $s$ -process element considered to be a necessary signature of the third dredge-up on the AGB (see discussion in § 5.1.3). Our optical spectra show that SS Vir is enhanced in other  $s$ -process elements, such as Ba, Y, and Zr (Barnbaum & Morris 1993), and therefore SS Vir likely achieved its carbon and  $s$ -process enrichment by mass transfer from a companion. V Hya, otherwise rich in  $s$  process elements, also appears to lack Tc based on the absence of a subordinate line in the red (see § 5.1.3 for a full explanation of this result). However, whereas the spectral broadening in V Hya varies over a photometric period, the spectrum of SS Vir remains unchanged; if the broadened spectrum of SS Vir is due to rotation, then its pulsation (as indicated by a photometric variation of 3.6 visible magnitudes from AAVSO; Mattei 1990) does not cause a significant change in angular velocity. The origin of the broadened spectrum of SS Vir is unexplained, and this star warrants further investigation.

SS Vir and S Aur provide evidence that some intrinsic spectral broadening in carbon stars exists, which is not unreasonable to expect. Line doubling may affect the derived widths in some Miras, but an additional mechanism seems required for SS Vir and S Aur. In § 5.2 we describe other mechanisms of broadening which might apply to these stars, such as differences in C/O abundance (Johnson, Luttermoser, & Faulkner 1988) or turbulence. What distinguishes V Hya from these stars is its large change of broadening with phase, not obviously

attributable to line doubling, combined with the large variation of radial velocity.

## 5. DISCUSSION

### 5.1. Variability Type and Evolutionary Status of V Hya

The variability of V Hya has implications for stellar evolution and can also put an upper limit on the rotation velocity, as compared with templates of the same type. Given its mass-loss rate and bipolar outflow, V Hya is possibly in a stage just before becoming a planetary nebula. The variability type of V Hya is of interest from an evolutionary standpoint since it is not at all clear whether carbon stars pass through a Mira phase before becoming proto-planetary nebulae. Also, if V Hya is a Mira it would constrain our estimate of the rotational broadening since we have shown in § 4.2 that Miras have some intrinsic spectral line broadening as compared with SR variables.

V Hya has characteristics normally attributed to both Miras and SR variables. For example, Miras are defined to vary by  $\geq 2.5$  visual magnitudes with a long, regular period. V Hya is classified by Mayall (1965) as an unusual SR variable with a total variation of close to  $3m_p$  over 533 days (AAVSO has recently measured a period of 529.2 days) and a secondary period, unusual for any type of LPV, of 6500 days with an amplitude of greater than  $6m_p$ . However, *JHK* photometry locates V Hya in the realm of Mira carbon stars (Feast & Catchpole 1985). Below, we discuss the mixture of spectroscopic properties that make classification of V Hya's variability type uncertain.

#### 5.1.1. Emission Lines

The emission lines present in optical spectra of V Hya are unusual. All Miras in our sample (a total of 22 stars with 63 total observations covering a variety of phases) observed near maximum light show very strong H $\alpha$  emission, whereas in V Hya, the H $\alpha$  emission line at its strongest (at  $\phi = 0$ ) is relatively weak, as it is in the few SR variables in our sample which show H $\alpha$  emission (seven out of 40 stars). In Figure 5, H $\alpha$  emission lines of two Miras, CZ Hya and RU Vir, are compared with the strongest H $\alpha$  line we have observed in V Hya. The spectra with solid lines are normalized to each other by assigning a common scale to the pseudocontinuum (i.e., the spectra are normalized to the strength of a single high point). The dashed-line spectra are magnifications of the same wavelength region.

Far into the blue region (3600–4700 Å) with low resolution (1.2–2 Å), Lloyd Evans (1991) has identified a number of strong atomic emission lines in V Hya near maximum light. He finds that S II, Ca II, Fe I, and Sr II are present in emission and at high velocities (blueshifted by  $\sim 150 \text{ km s}^{-1}$  from the rest velocity of V Hya). In addition, he reports that the higher Balmer transitions (H $\delta$  and above) have an absorption component and suggests that these arise from a companion. Although we find in our high-resolution spectra that H $\alpha$  has no absorption feature at any phase, the luminosity of the carbon star would obscure any warm companion at this redder wavelength.

In the search for evidence of chromospheres around AGB stars, a number of carbon stars, including SR and Mira variables, have been observed over the years with *IUE*, with the result that the few stars with detectable Mg II emission are all SR or Lb variables (see Johnson & Luttermoser 1987 for a list of carbon stars successfully observed with *IUE*). In 1988 we observed V Hya with the *IUE* low-resolution spectrograph



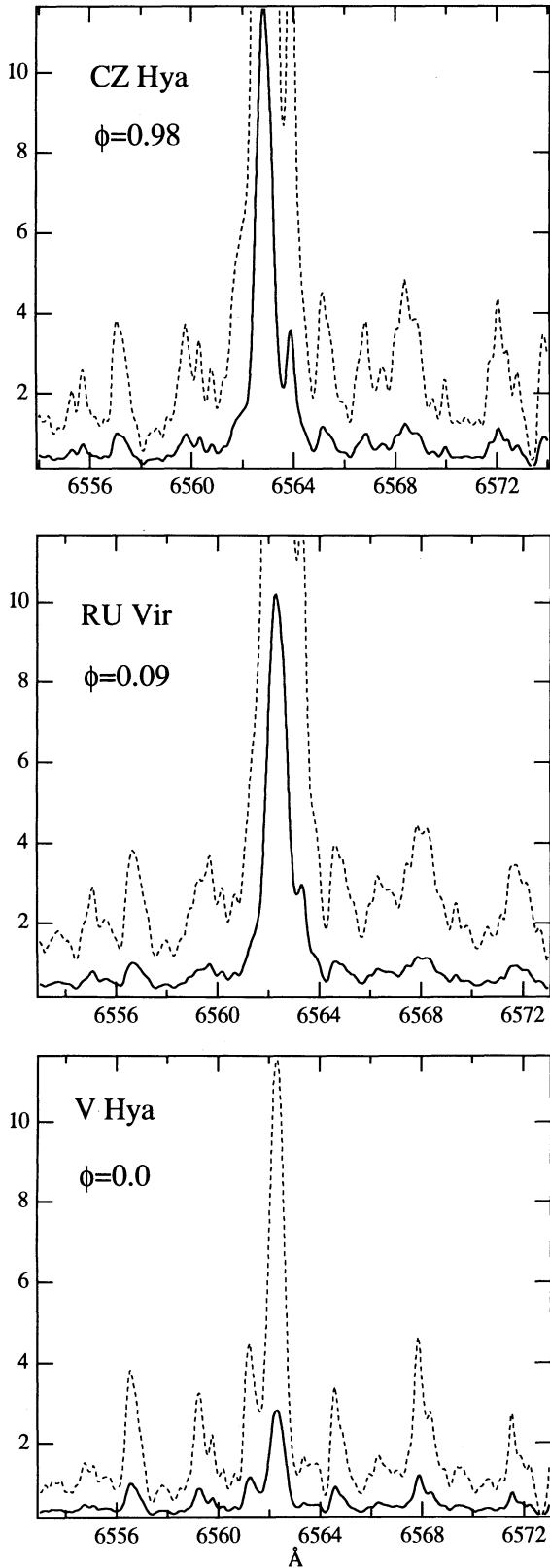


FIG. 5.— $H\alpha$  emission in Mira carbon stars near maximum light. Each spectrum was normalized to the strength of the feature near 6556 Å, the adopted pseudo continuum. The y-axis represents the relative intensity of the solid-line spectra, with the pseudocontinuum of each star normalized to the same value. The dashed lines show the enlarged spectra, showing the structure of neighboring absorption line features, all plotted from 0 to 3.0 on the relative intensity scale.

(see Fig. 6) and successfully detected the blended Mg II doublet  $\lambda\lambda 2795.56$  and  $2802.698$  with an integrated flux of  $1.6 \times 10^{-13}$  ergs  $s^{-1} cm^{-2}$ , within a factor of 2 below that observed in other carbon star SR and Lb variables (Luttermoser & Brown 1992). If V Hya is an AGB star and a Mira variable, then our detection of Mg II makes V Hya the first carbon star Mira with observable emission in the ultraviolet.

#### 5.1.2. Absorption Line Velocities

The behavior of absorption line velocities in V Hya is not typical of either SR, Lb, or Miras, yet characteristics of each are present. The radial velocities of strong atomic absorption lines (such as those of K I, Mg Ib and Li I) in the atmosphere of a typical carbon star Mira, can differ by as much as  $30 km s^{-1}$  and demonstrate a large variation with phase, with the largest dispersion at maximum light and smallest at minimum light. However, atomic line velocities of SR and Lb variables typically differ from line to line by only  $5-8 km s^{-1}$ , and the variation with phase shows no consistent pattern (Barnbaum 1992a). Figure 7 shows the atomic and molecular line velocities versus photometric phase for V Hya and for a typical Mira and SR variable. (Note that the velocity scale is the same in each plot and that the symbol labeled “molecular” refers to the cross-correlation velocity over 3000 Å of the optical spectral window and is presumably a measure of the statistical average of the bulk atmospheric motion.)

The behavior of absorption line velocities in CZ Hya is typical of other Miras in our sample for which we have adequate phase coverage. The molecular lines of the Mira CZ Hya

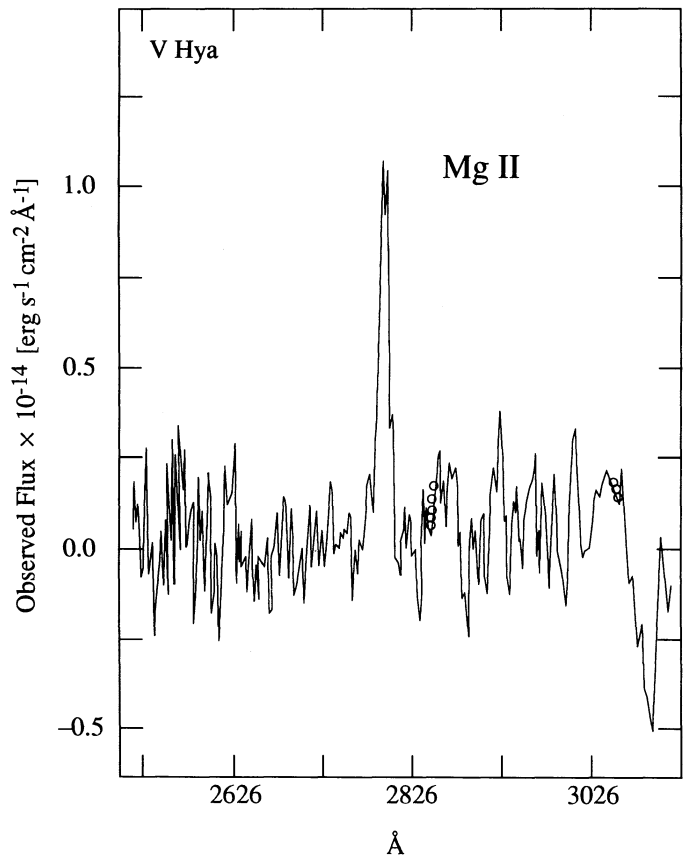


FIG. 6.—IUE spectrum (LWP) showing the Mg II emission line observed 1988 November 24. The small circles show where pixel zapping removed anomalous spikes.

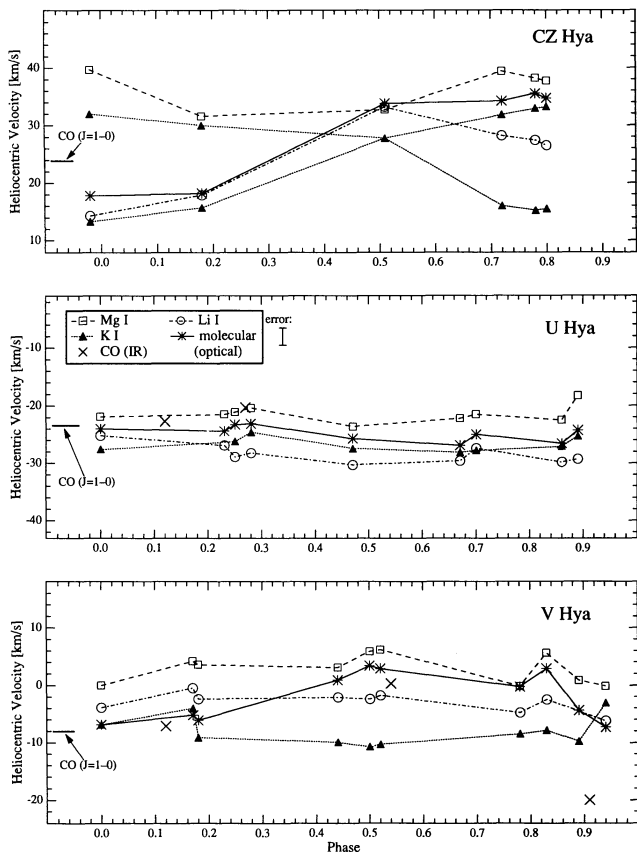


FIG. 7.—Heliocentric radial velocity vs. phase for a Mira (CZ Hya), SR variable (U Hya), and V Hya. The “molecular (optical)” velocity refers to the cross-correlated velocity of  $\sim 30$  spectral orders with a template and represents a statistical average of the atmospheric motion, which is dominated by molecular absorption lines (mostly CN). The atomic velocities are: Li  $\lambda 6707.84$ , Mg  $\lambda 5183.61$ , and K  $\lambda 7698.96$ . Note that K I is doubled in CZ Hya and the two components merge near minimum light. The error for each measurement is  $\pm 1.5 \text{ km s}^{-1}$ . The radio (114 GHz) emission line of circumstellar CO ( $J = 1-0$ ) is indicated on the left. For U Hya and V Hya, the infrared ( $2 \mu\text{m}$ ) absorption lines of the CO vibration lines from Fourier transform spectra are indicated.

at minimum light (see Fig. 7a) are single and have a velocity of  $\sim 32 \text{ km s}^{-1}$ , but doubling occurs as the star approaches maximum light and the cross-correlation velocity shifts to  $18 \text{ km s}^{-1}$ . At this time the cross-correlation function becomes asymmetric with a weaker peak near  $32 \text{ km s}^{-1}$ . Typical of SR and Lb variables in general, the molecular and atomic line velocities in the SR variable U Hya (Fig. 7b) not only remain steady throughout the light phase but they are all close to each other. The velocity pattern of V Hya, however, intermediate between typical SR and Mira behavior. V Hya’s atomic velocities are closer to each other than in Miras but somewhat more dispersed than in typical SR variables (Fig. 7c). Also, V Hya shows no splitting of molecular lines or even of K I as typically occurs in Miras and occasionally in SR and Lb variables. The behavior of the atomic and molecular absorption lines in V Hya has characteristics of both Mira and SR variables, having neither the pattern found in Miras nor the close agreement of velocities as in SR variables.

The optical molecular velocity of V Hya is always somewhat redshifted from the center-of-mass velocity, which is typical of Miras, both oxygen and carbon rich (oxygen rich, Reid & Dickinson 1976 and Barbier et al. 1988; carbon rich, Barn-

baum 1992b). On the other hand, the velocities of SR and Lb variables can be either blueshifted or redshifted from rest velocity (Barnbaum 1992b), as one would expect as a consequence of atmospheric pulsations. The center-of-mass velocity is easily measured from the circumstellar radio emission line CO ( $J = 1-0$ ), and these velocities appear in Figure 7, as lines drawn on the left of each plot. Scattering off dust grains in the circumstellar envelopes of Miras has been suggested as the cause of the systematic redshift of measured optical velocities (Romanik & Leung 1981), and the  $12 \mu\text{m}$  (IRAS) to  $2 \mu\text{m}$  (Two Micron Sky Survey [TMSS]) flux ratio places V Hya in the region of the dusty Mira variables. But scattering would only account for a few kilometers per second, and some Miras have offsets as large as  $15 \text{ km s}^{-1}$ . The redshift phenomenon in Miras is likely a combination of dust-scattering effects and opacity changes during a pulsation period such that the optical light always samples infalling material (Hinkle, Scharlach, & Hall 1984), and this is consistent with Miras having deeper amplitudes of pulsation than the SR or Lb variables.

Included in Figure 7 (middle and bottom) are velocities of the CO fundamental vibration transitions near  $2 \mu\text{m}$  measured with the Fourier transform spectrometer on the 4 m telescope at Kitt Peak National Observatory. These data are part of a larger study that will be presented in detail in a separate paper (Barnbaum & Hinkle 1995). These transitions arise lower in the atmosphere than the optical lines (see Hinkle 1978). In V Hya, the infrared CO velocities vary in the same direction as the optical cross-correlation velocities, while typically in SR variables the infrared CO velocity remains fairly steady with phase (Barnbaum & Hinkle 1994, 1995).

The radial velocity variations of V Hya are not those of a typical Mira or SR variable but rather somewhere in between, as Figure 7 demonstrates. If we collate the velocity information we have obtained on V Hya, the most reasonable conclusion appears to be that its variability type is neither classically Mira nor SR and that it is possibly an object in transition.

### 5.1.3. Elemental Abundances and Evolutionary Status

Since V Hya is carbon-rich and in addition has a dusty circumstellar envelope, it has been generally assumed that it is on the AGB. However, the carbon enhancement and mass loss might be driven by a stellar merger rather than by the red giant having already reached the superwind AGB phase. The inversion of C/O might then be the result of a dredge-up caused by tidal interactions when the companion was engulfed by the primary star, instead of being caused by the usual instabilities that take place during a star’s tenure on the AGB.

The atmospheres of carbon stars on the AGB are enriched in *s*-process elements as a consequence of the third dredge-up, which is also responsible for carbon enrichment (see Iben & Renzini 1983). We have measured the relative strength of *s*-process elements in the carbon stars of our sample (Barnbaum & Morris 1993). Not surprisingly, all the stars (except for the *J*-types) are enhanced in *s*-process elements such as Ba, Y, and Zr, as is the atmosphere of V Hya. An element that traces the recent dredge-up of *s*-process elements is  $^{99}\text{Tc}$  (see Little et al. 1987). Tc is expected to be present in all AGB carbon stars, since its half-life of  $7 \times 10^5 \text{ yr}$  approaches the lifetime of a carbon star on the AGB. If *s*-process elements are present, but not Tc, then the carbon star must have acquired its peculiar abundances from mass transfer by a companion, or by some mechanism other than the third dredge-up (Little et al. 1987; Little-Marenin 1989). Therefore, the presence of Tc is an

important indicator of the evolutionary status of a star. In S stars (normally AGB stars with  $C/O \sim 1$ ) it has been shown that a lack of Tc is associated with mass transfer from a companion (Brown et al. 1990; Jorissen et al. 1993; Johnson, Ake, & Ameen 1993). If mass transfer from a companion has occurred, then V Hya is not on the AGB, and its evolution is being directed by interaction with its companion.

Determining the presence of Tc is not an easy task. The strong resonance lines in the blue (near 4297 Å) are difficult to observe since carbon stars are very faint in this spectral region, and line blending here adds to the problem. Tc detections or nondetections were previously known for only 16 carbon stars from the work of Little et al. (1987). We have identified a subordinate line of  $^{99}\text{Tc}$  in the red that traces the presence or absence of the blue resonance lines for the 16 previously observed stars. If this line at 6085.22 Å can be trusted as a test of the presence of Tc, then Tc does not appear to be present in the atmosphere of V Hya, an indication that this star has not undergone a normal ascent along the AGB.

### 5.2. Alternative Sources of Broadening

In conducting our broadening analysis, we have implicitly assumed that the broadening results from rotation. The effect of weak line doubling on spectral broadening was discussed in § 4.2. Although this possibility cannot be dismissed, we have no observational evidence for it in V Hya with the resolution used in this study. Fourier transform spectra (Barnbaum & Hinkle 1994, 1995) of the 2  $\mu\text{m}$  region observed at  $\phi = 0.13$  and 0.91 suggest the possibility of unresolved doubling of fundamental and overtone vibrational lines of CO with a resolution of 65,000 (0.3 Å or 4.6  $\text{km s}^{-1}$  at 2  $\mu\text{m}$ ). These transitions arise lower in the atmosphere than the optical lines and have been known to show extreme doubling (component separation of 30  $\text{km s}^{-1}$ ) in the Mira S star  $\chi$  Cyg (Hinkle et al. 1982). Infrared Fourier transform spectra of one other carbon star Mira in our sample, S Cep, show strong line doubling just before maximum light, from  $\phi = 0.9$  to 0.0, with features separated by 21  $\text{km s}^{-1}$  (Barnbaum & Hinkle 1995). Yet our optical observations of S Cep near maximum at  $\phi = 0.90$  show only weak line splitting, indicating that line doubling, when present, has greater velocity separation in the deeper infrared layer than in the material higher in the atmosphere that is sampled by optical spectra. In V Hya, at  $\phi = 0.91$ , the infrared CO lines show weak, unresolved doubling, with a maximum separation of  $\sim 10 \text{ km s}^{-1}$ , based on the asymmetry of the cross-correlation profile. Line doubling in the infrared, if real, is weak in V Hya. It is likely then that any line doubling in the optical spectra is just at our resolution and is therefore unlikely to contribute to the observed broadening in V Hya.

There are two other alternative broadening mechanisms that warrant consideration: turbulence and opacity, and both of these may depend on photometric phase in stars with a large amplitude of pulsation. For example, the atmospheres of Cepheid and RR Lyrae variables are apparently characterized by a phase-dependent turbulent broadening (Benz & Mayor 1982; Benz & Stellingwerf 1985). It has been shown that turbulence in the atmosphere of pulsating Cepheids causes spectral broadening of 5–12  $\text{km s}^{-1}$  and that the lines are broader when the star is near minimum radius and narrowest near maximum radius. However, the radial velocity variation in these stars, due to the pulsational motion of the atmosphere, is on the order of 50  $\text{km s}^{-1}$ , whereas the radial velocity variation of V Hya is only 11  $\text{km s}^{-1}$ . Therefore, it seems unlikely that 11

$\text{km s}^{-1}$  spectral broadening would be caused by turbulence due to pulsation in V Hya.

Opacity changes due to temperature variation might affect the line profiles of molecular species. However, we do not believe that this mechanism is important in V Hya because V Hya is alone in our sample in having such obvious phase-dependent broadening not caused by weak line doubling. A large opacity in the photospheric absorption lines would broaden them and enhance their wings. If a large line opacity is the predominant broadening mechanism, then it must be much larger in V Hya than in any of the other stars studied. This might be arranged if the V Hya line formation region is substantially cooler than that of other stars (Luttermoser & Brown 1992), but in fact this does not appear to be the case (X Cnc, e.g.; Kahane et al. 1988). Alternatively, the molecular column densities down to the layer where the continuum opacity exceeds unity might be larger in V Hya than in other stars, but in order to broaden all of the lines substantially, the column density would have to be orders of magnitude larger than usual, which is unlikely.

Luttermoser & Brown (1992) suggest that a difference of only 200 K in effective temperature between templates and V Hya would be significant to the line opacities; in addition, since a greater C/O abundance for a given effective temperature ( $T_{\text{eff}}$ ) creates a deeper cooler layer broadening effects might arise from this combination of temperature-abundance differences (Johnson et al. 1988). We have observed 25 of the 30 stars for which C/O abundances have been measured by Lambert et al. (1986), of which V Hya is one. We have used these 24 stars of Lambert et al. as template comparisons to V Hya. These stars vary in C/O ratio from 1.014 to 1.76 and in  $T_{\text{eff}}$  from 2450 to 3030 K. Five of these 24 stars are within 50 K of V Hya, and yet all need to be broadened by some amount to fit the spectrum of V Hya at any phase (see Table 7). The possibility that inappropriate templates account for the apparent line broadening in V Hya, as suggested by Luttermoser & Brown, would require that the effective temperature and C/O measurements be very inaccurate for V Hya. Indeed, if V Hya is not on the AGB, then the calculation of effective temperature, which depends in part on the assumed evolutionary status in the model atmosphere, might be in error.

Rotation as the cause of phase-dependent spectral broadening in V Hya cannot be unambiguously proved by our treatment here. However, we can point to the consistency of everything we know about V Hya when V Hya is compared

TABLE 7  
C/O AND  $T_{\text{eff}}$  FOR CARBON STARS COMPARED TO V HYA<sup>a</sup>

Template	$T_{\text{eff}}$ (K)	C/O	Rotation Velocity $v \sin i$ Fit to V Hya ( $\text{km s}^{-1}$ )	$\phi$ of V Hya <sup>b</sup>
X Cnc .....	2600	1.14	5.9 12.7	0.50 0.83
W Ori .....	2680	1.16	6.7 14.5	0.50 0.83
V Aql .....	2610	1.25	12.3 15.1	0.17 0.78
VX And .....	2700	1.76	14.2	0.83
Y Tau .....	2600	1.04	14.5	0.83

<sup>a</sup> C/O and  $T_{\text{eff}}$  from Lambert et al. 1986. For V Hya, C/O = 1.05 and  $T_{\text{eff}} = 2650 \text{ K}$ .

<sup>b</sup> The phase,  $\phi$ , indicates maximum light at  $\phi = 0.0$  and minimum light at  $\phi = 0.45$ .

with other carbon stars of all types, and we conclude that the broadening is *most likely* due to the rotation of V Hya at near breakup speed. The changes of  $v \sin i$  with phase are consistent with radial pulsations in the fundamental mode and the consequent periodic change of the moment of inertia.

### 5.3. Pulsation of V Hya

The hypothesis that V Hya is rotating allows us to use the combination of radial velocity and rotational velocity data to determine the equilibrium size of the star. First, we integrate the photospheric velocity through a light cycle:

$$\frac{dr}{dt} = -pV_{\text{rad}}(t),$$

where  $V_{\text{rad}}$  is the measured radial velocity with time and  $p$  is the limb-darkening correction factor equal to 1.37 (Cox 1980, p. 27; Parsons 1971). We assume that  $V_{\text{rad}}(t)$  varies sinusoidally over the 530 day period ( $P$ ) with a full amplitude of  $V_0 = 10.7 \text{ km s}^{-1}$  and find that the displacement of the photosphere between minimum and maximum radius amounts to  $\Delta R = R_{\text{max}} - R_{\text{min}} = pV_0 P/2\pi = 1.0 \times 10^{13} \text{ cm}$ . The radii  $R_{\text{max}}$  and  $R_{\text{min}}$  are further constrained by the measured values of  $v \sin i$  and the conservation of angular momentum. We assume that both the stellar density structure and the distribution of specific angular momentum, both axisymmetric, change homologically during the pulsation cycle. These assumptions lead to the simple relation

$$R_{\text{min}} v_{\text{rot}}(R_{\text{min}}) = R_{\text{max}} v_{\text{rot}}(R_{\text{max}}),$$

where  $v_{\text{rot}}$  is the equatorial rotation velocity. Then, attributing the variation of the stellar line width entirely to rotational broadening and changing from  $v_{\text{rot}}(R_{\text{max}}) \sin i = \sim 9$  to  $v_{\text{rot}}(R_{\text{min}}) \sin i = \sim 17.5 \text{ km s}^{-1}$  during the pulsation (as inferred from SR variables), we can solve for  $R_{\text{min}}$ ,  $R_{\text{max}}$ , and the equilibrium radius,  $R_{\text{eq}}$ :

$$R_{\text{max}} = \Delta R / [1 - v_{\text{rot}}(R_{\text{max}})/v_{\text{rot}}(R_{\text{min}})] = 2.1 \times 10^{13} \text{ cm},$$

$$R_{\text{eq}} = R_{\text{max}} - \Delta R/2 = 1.6 \times 10^{13} \text{ cm},$$

$$R_{\text{min}} = 1.1 \times 10^{13} \text{ cm}.$$

This value of  $R_{\text{eq}}$  is within a factor of about 2 of a reasonable equilibrium value ( $\sim 400 R_{\odot}$ ) for a carbon star on the AGB. If, instead, we use the values of  $v_{\text{rot}}(R_{\text{max}}) \sin i$  and  $v_{\text{rot}}(R_{\text{min}}) \sin i$  taken by using Mira variables as templates (4.5 and 13.5  $\text{km s}^{-1}$ , respectively), then  $R_{\text{eq}} = 1.0 \times 10^{13} \text{ cm}$ ,  $R_{\text{max}} = 1.5 \times 10^{13} \text{ cm}$ , and  $R_{\text{min}} = 5 \times 10^{12} \text{ cm}$ . This value of  $R_{\text{eq}}$  is a factor of about 5 or 6 smaller than is believed to be appropriate for an AGB star, so either V Hya is not on the AGB or the Mira templates are inapplicable and misleading due to their intrinsically large line widths.

The magnitude of total radial excursion that we infer strongly suggests that the mode of pulsation is equivalent to the fundamental mode. By "equivalent," we recognize that rotation leads to a deviation from spherical symmetry that will modify the character of the fundamental mode (see Tassoul 1978). The magnitude of the velocity of pulsation is comparable to the rotation velocity in this star, so we might imagine that Coriolis forces come into play and give rise to latitude-dependent atmospheric circulation patterns which could affect the mass loss (Morris & Barnbaum 1993).

### 5.4. Detached Binary or Common Envelope Evolution

The angular momentum of the envelope of V Hya is far in excess of that which could have been present in a single-

precursor main-sequence star. To illustrate this, consider a 1.5  $M_{\odot}$  star rotating with breakup velocity during its main sequence phase. By conservation of angular momentum, the expansion to the radius of a typical AGB star would slow the rotation to  $2 \text{ km s}^{-1}$ . A rotation velocity of 10–18  $\text{km s}^{-1}$  must have its origins from without. Our hypothesis that the broadening is owed to rotation necessitates the presence of a binary companion that has tidally spun up the giant. In principle, the binary system could be in either a detached or common envelope configuration.

A detached binary configuration has been favored by some investigators as a means of explaining the high-velocity gas motions in this system (Sahai & Wannier 1988; Lloyd Evans 1991) in terms of a polar-directed flow arising from an accretion disk attached to V Hya's putative companion (Morris 1987). Such flows, however, have other potential explanations (see, e.g., § 5.5). A problem with a detached configuration is that, even in the most favorable case where the rotation of the giant is synchronous with the companion's orbit, the observed rotation rate appears to be too large unless the companion is close to the surface of V Hya (i.e., in a semidetached state) and the inclination of the orbit is  $\sim 90^{\circ}$ . However, the radio data (Kahane et al. 1995) suggest that the symmetry plane of the outflowing envelope is inclined by about  $30^{\circ}$ , so one would have to abandon the rather natural notion that the binary's orbital plane defines the symmetry plane of the outflow.

The detached binary hypothesis also encounters other serious difficulties. If a close companion is present, as suggested by Lloyd Evans (1991), then it is reasonable to estimate that at least  $\sim 10\%$  of the mass lost from V Hya is being accreted onto the companion (e.g., Jura & Helfand 1984). If we assumed that the inevitable accretion disk is optically thick, then the flux of the disk can be approximated by a blackbody and set equal to the dissipation rate due to viscous forces. As shown in Frank, King, & Raine (1985), the temperature of the disk near the companion's surface is given by  $T_* \sim [3GM_*\dot{M}/(8\pi\sigma R_*^3)]^{1/4} \sim 9000 \text{ K}$ . The accretion luminosity is approximated as half the luminosity of the disk  $\sim GM_*\dot{M}/(2R_*)$  (see Frank et al. 1985, p. 832), which leads to a predicted flux of  $\sim 2.2 \times 10^{-13} \text{ ergs s}^{-1} \text{ cm}^{-2} \text{ \AA}^{-1}$  for an  $\sim 1 M_{\odot}$  companion accreting  $\sim 10^{-7} M_{\odot} \text{ yr}^{-1}$  (10% of the mass-loss rate of V Hya) at a source distance of 340 pc (Claussen et al. 1987). An upper limit on the continuum flux of  $\sim 3.5 \times 10^{-15} \text{ ergs s}^{-1} \text{ cm}^{-2} \text{ \AA}^{-1}$  from our IUE spectrum (see Fig. 6) is not consistent with the presence of a main-sequence companion if the ultraviolet extinction is not greater than about 6 mag, or if at least  $\sim 1\%$  of the flux generated in the disk is scattered out of the nebula by dust in the bipolar lobes. A compact companion would generate even more ultraviolet luminosity and can be even more strongly excluded.

We can further constrain the possible companion by considering the radial velocity variation of V Hya. The higher order Balmer absorption lines described by Lloyd Evans (1991) suggest an early G or F companion, implying a mass of 1–1.5  $M_{\odot}$  or possibly a white dwarf. We have shown that the radial velocity variations of V Hya have the same period as the light curve, 530 days. If we take a mass of 1.5  $M_{\odot}$  for the companion and an orbital period of 530 days, then we would expect a radial velocity amplitude of (40–60)  $\text{km s}^{-1} \sin i$  (for inclination angle  $i$ ), which for  $i = 30^{\circ}$ – $45^{\circ}$  is significantly larger than the  $\sim 12 \text{ km s}^{-1}$  amplitude that we observe in V Hya and which we attribute predominantly to pulsation. Furthermore, if we do not constrain the companion to be in close proximity, that is, if V Hya is not rotating and there is no excess angular

momentum in its envelope, then  $1.5 M_{\odot}$  for the companion with a total radial velocity variation of  $12 \text{ km s}^{-1}$  gives a separation of the binary near  $3200 R_{\odot}$ , or  $\sim 15 \text{ AU}$ , and an orbital period of 13,600 days. This separation is too large to cause such a pronounced collimation of the outflow from V Hya if the ratio of mass in the bipolar flow that in the otherwise spherical part of the flow is more than  $\sim 10\%$ , which it most likely is (Kahane et al. 1995). We suggest that the key to understanding the Balmer lines may lie in studying their velocities. If they do not show the periodic variations expected of an orbiting companion, they might be understood in the framework of the polar jets.

One potential piece of evidence for a disk and/or companion must still be explained, however, the apparent blue continuum reported by Lloyd Evans (1991). A proper modeling of the continuum is needed to distinguish between an interpretation in terms of scattering in V Hya's bipolar lobes and one in terms of direct but partially obscured emission from a companion, but the intensity and proper shape of the continuum is not clear from Lloyd Evans's Figure 1 since the spectrum shown is a sum of several different epochs and is not quantified.

We suggest that V Hya is more likely to be in a common envelope configuration. With a sufficiently massive companion (at least a few tenths of a solar mass), the unusually high rotation of V Hya is readily accounted for; the equatorial velocity may attain the limiting value of  $\sim 30 \text{ km s}^{-1}$  at the equator, at which matter is extruded into a Keplerian disk. If V Hya is a common envelope binary, as we suggest, then it can be distinguished from a detached system using the light curve. The nonaxisymmetric distortions of the giant in a detached system in corotation should be revealed as a variation in the light curve at the period of rotation. This would be one of the more promising ways to investigate the rotation of this system, if it is detached. In a common envelope system, the envelope rotation could not keep up with the rotation of its cores, and if the common envelope timescale is sufficiently long, the envelope would take on an oblate, axisymmetric distortion.

### 5.5. Rotational Driving of a High-Velocity Polar Flow

The high velocities reported by Sahai & Wannier (1988) and Lloyd Evans (1991) probably require a mass ejection mechanism other than radiation pressure on dust grains. For example, a model analogous to that of Shu et al. (1988) for bipolar flows from rapidly rotating protostellar systems might be applied to evolved, mass-losing systems displaying bipolarity (Morris 1990). In the case of a common envelope system, the orbital decay of the stellar cores provides a constant supply of angular momentum which must be shed by mass loss if the envelope is already at its breakup speed. Then, if the magnetic field lines have the appropriate geometry, that is, if they are open field lines which form an angle of at least  $30^{\circ}$  with respect to the star's rotation axis, a fast, centrifugally driven, bipolar, magnetic wind can be established.

Such a mechanism for driving bipolar winds from evolved stars was considered recently by Najita (1993), who argues that substantial magnetic fields would be generated in evolved, rapidly rotating giants by a dynamo mechanism resulting from the coupling of convection and rotation. Then, if the star is rotating at the marginal breakup speed, the X-celerator mechanism, which was developed to explain bipolar outflows in protostellar systems (Shu et al. 1994), can be applied. According to this hypothesis, mass lost at the stellar equator is centrifugally flung out along field lines, and it is constrained to follow those

field lines as they eventually converge upon, or wrap around, the polar direction.

An alternative mechanism for generating high-velocity polar flows in common envelope configurations was proposed by Soker (1992). He notes that the rapid rotation engendered by the angular momentum passed from the companion to the AGB star's envelope would lead to a strong deformation of the stellar surface. Because of this deformation, mass loss from the stellar surface is aimed predominantly along the symmetry axis, forming the polar jets. The broad, conical outflow centered on the symmetry axis in V Hya (Kahane et al. 1995), where the polar jets are presumably located, is consistent with this picture.

### 5.6. A speculation on the Nature of the 6500 Day Secondary Period

The rotation and fundamental-mode pulsation periods of V Hya have comparable values, inasmuch as the rotation and pulsation velocities are similar. However, they are not identical. For the equilibrium radii derived above in § 5.2, the rotation period at the surface of the star is  $878 \sin i$  or  $808 \sin i$  days (given the alternative measured values of  $\langle v_{\text{rot}} \rangle \sin i = 13.25$  or  $9 \text{ km s}^{-1}$ , respectively). The beat frequency between rotation, with a 529.3 day period, and pulsation will therefore correspond to a 6500 day period if  $i = 41^{\circ}$  or  $45^{\circ}$ . We therefore suggest that the interaction between rotation and pulsation be considered as the source of the secondary period. Of course, this interaction is complex, and we do not attempt here to characterize its nature, but only to point out that it is numerically plausible.

If these values for the inclination are adopted, then the equatorial rotation velocities at  $R_{\text{min}}$  are  $26.7$  and  $18.9 \text{ km s}^{-1}$ , respectively, for the two cases considered. These rather high rotation velocities approach the breakup velocities of the star:  $v_{\text{breakup}} = (GM_{*}/R_{\text{min}})^{1/2} = 35$  or  $52 \text{ km s}^{-1}$ , for each value of  $R_{\text{min}}$  respectively, where  $M_{*}$  is the mass of V Hya. In fact, since we have not considered the oblate distortion of the star caused by rotation, it is possible that the equatorial velocity is essentially identical to the breakup velocity. If so, then the conditions for the centrifugally driven wind models described in § 5.5 are met, and these models become particularly attractive for explaining the bipolar morphology of V Hya's wind.

## 6. CONCLUSIONS

The broadened spectrum and bipolar outflow of V Hya show it to be an exceptional carbon star. By measuring the photospheric velocity and by carrying out a broadening analysis at many epochs spanning several pulsational periods, we have noted the rise and fall of the photosphere with approximately the light-curve phasing expected for a radially pulsating star. In addition, we have found that the amount of broadening depends on the phase of the light curve, with a relationship consistent with that expected for a rapidly rotating star that conserves angular momentum as it pulsates. While line-broadening mechanisms other than rotation—notably macroturbulence and line opacity—have been considered and cannot be definitively ruled out, we find that rotation is by far the most compelling: (1) it accounts nicely for the phase relationships between the light curve, the photospheric velocity, and the line broadening, (2) it defines a symmetry axis for the bipolar flow and gives rise to plausible mass ejection mechanisms which can, in principle, account for the high observed velocities in the flow, and (3) it allows one to

understand why V Hya is essentially unique among the 86 carbon stars which we have studied, on the basis that stars with such rapid rotation should be in a rather brief evolutionary stage.

Application of basic mechanics to the magnitude of the photospheric and rotational velocity changes during the light cycle, coupled with the assumptions that the changes in the structure of the atmosphere during pulsation are spherically symmetric and homologous, permits us to infer reasonable values for the equilibrium stellar radius (about 1 AU) and the radial range of the pulsational excursions (50% about equilibrium). Allowing for a nonperpendicular orientation of the rotation axis with respect to the line of sight, we conclude that V Hya is rotating at near breakup speed, as required by some models of bipolar outflows. The magnitude of the radial motions also suggests that V Hya is pulsating in its fundamental mode, although the character of the fundamental mode would be strongly affected by rotation; i.e., it would not be spherically symmetric. Noting further that the periods of rotation and pulsation are comparable in magnitude, we speculate that the secondary 6500 day period of V Hya is owed to an interaction between these motions.

The evolutionary status of V Hya is a particularly interesting question. First, it cannot be unambiguously assigned to any particular variable category (i.e., Mira or SR variable) because it appears to have intermediate properties, or properties characteristic of both types. Second, the absence of a red technetium line which we have observed in other carbon stars, even though other *s*-process elements are enhanced, suggests that V Hya is not undergoing a normal ascent of the AGB. Third, if V Hya is indeed rotating at near breakup speed, then the pos-

sible scenarios for generating it are very limited. The angular momentum inferred for the stellar atmosphere could only have come from a binary companion that is either in a semidetached or common envelope configuration. The lack of evidence for orbital motions in the photospheric velocity measurements, the absence of a hot continuum from an accretion disk around any external companion, and the sheer quantity of angular momentum in the atmosphere and presumably in the bipolar flow all lead us to the conclusion that V Hya is most likely to be a common envelope binary. The rarity of systems such as V Hya is consistent with the shortness expected for the lifetime of the common envelope stage. Indeed the finding of even this single object, more or less stable in luminosity through this century (Mayall 1965), would place an interesting lower bound on the lifetime of the common envelope stage.

Further progress in understanding this potentially key system will require continued detailed monitoring of the photospheric velocity field, perhaps in the infrared. Interferometric studies in the infrared will also be important for determining whether it indeed has a binary companion, for determining whether a disk is important in this system, and for determining the shape of the star. If V Hya can be shown to be a common envelope system, then it will serve as the Rosetta stone for understanding this brief but crucial stage of stellar evolution.

We are grateful to M. Jura for helpful discussions and insightful comments on the manuscript. We also thank J. Najita for enlightening discussions of theoretical treatment. This research has been partially supported by NSF AST 92-18157 to UCLA.

## REFERENCES

- Barbier, M., Mayor, M., Mennessier, M. O., & Petit, H. 1988, *A&AS*, 72, 463  
 Barnbaum, C. 1992a, *AJ*, 104, 1585  
 ———. 1992b, *ApJ*, 385, 694  
 ———. 1994, *ApJS*, 90, 317  
 Barnbaum, C., & Hinkle, K. 1994, in *Science with Astronomical Near Infrared Surveys*, ed. N. Epchtein, A. Omont., & W. B. Burton (Dordrecht: Kluwer), 151  
 ———. 1995, *AJ*, in press  
 Barnbaum, C., & Morris, M. 1993, *BAAS*, 25, 876  
 Benz, W., & Mayor, M. 1982, *A&A*, 111, 224  
 Benz, W., & Stellingwerf, R. F. 1985, *ApJ*, 297, 686  
 Brown, J. A., Smith, V. V., Lambert, D. L., Dutchover, E., Jr., Hinkle, K. H., & Johnson, H. R. 1990, *AJ*, 99, 1930  
 Carroll, J. A. 1933, *MNRAS*, 93, 478  
 Claussen, M. J., Kleinmann, S. G., Joyce, R. R., & Jura, M. 1987, *ApJS*, 65, 385  
 Cox, J. P. 1980, *Theory of Stellar Pulsation* (Princeton: Princeton Univ. Press)  
 Feast, M. W., & Catchpole, R. M. 1985, in *Cool Stars with Excesses of Heavy Elements*, ed. M. Jасhek & P. C. Keenan (Dordrecht: Reidel), 113  
 Frank, J., King, A. R., & Raine, D. J. 1985, *Accretion Power in Astrophysics* (New York: Cambridge Univ. Press)  
 Goodrich, R. W., & Veilleux, S. 1988, *PASP*, 100, 1572  
 Gray, D. F. 1976, *The Observation and Analysis of Stellar Photospheres* (New York: Wiley)  
 Hinkle, K. H. 1978, *ApJ*, 220, 210  
 Hinkle, K. H., & Barnes, T. G. 1979, *ApJ*, 234, 548  
 Hinkle, K. H., Hall, D. N. B., & Ridgway, S. T. 1982, *ApJ*, 252, 697  
 Hinkle, K. H., Scharlach, W. W. G., & Hall, D. N. B. 1984, *ApJS*, 56, 1  
 Iben, I., Jr., & Livio, M. 1993, *PASP*, 105, 1373  
 Iben, I., Jr., & Renzini, A. 1983, *ARA&A*, 21, 271  
 Johnson, H. R., Ake, T. B., & Ameen, M. M. 1993, *ApJ*, 402, 667  
 Johnson, H. R., & Luttermoser, D. G. 1987, *ApJ*, 314, 329  
 Johnson, H. R., Luttermoser, D. G., & Faulkner, D. R. 1988, *ApJ*, 332, 421  
 Jorissen, A., Frayer, D. T., Johnson, H. R., Mayor, M., & Smith, V. V. 1993, *A&A*, 271, 463  
 Jura, M., & Helfand, D. J. 1984, *ApJ*, 287, 785  
 Jura, M., & Kleinmann, S. G. 1992, *ApJS*, 79, 105  
 Kahane, C., Audinos, P., Barnbaum, C., & Morris, M. 1993, in *Mass Loss on the AGB and Beyond*, ed. H. Schwarz (CTIO/ESO Workshop, Chile) (Munich: ESO), 437  
 ———. 1995, in preparation  
 Kahane, C., Maizels, C., & Jura, M. 1988, *ApJ*, 328, L25  
 Kerschbaum, F., & Hron, J. 1992, *A&A*, 263, 97  
 Kholopov, P. N., ed. 1985 *General Catalog of Variable Stars* (4th ed.; Moscow: Nauka)
- Lambert, K. L., Gustafsson, B., Eriksson, K., & Hinkle, K. H. 1986, *ApJS*, 62, 373  
 Little, S., Little-Marenin, I. R., & Bauer, W. H. 1987, *AJ*, 84, 1374  
 Little-Marenin, I. 1989, in *IAU Colloq. 106, Evolution of Peculiar Red Giant Stars*, ed. H. R. Johnson & B. Zuckerman (New York: Cambridge Univ. Press), 131  
 Little-Marenin, I. R., Benson, P. J., & Cadmus, R. R., Jr. 1993, in *Astrophysical Masers*, ed. A. W. Clegg & G. E. Nedduhla (New York: Springer), 295  
 Lloyd Evans, T. 1991, *MNRAS*, 248, 479  
 Luttermoser, D. G., & Brown, A. 1992, *ApJ*, 384, 634  
 Mattei, J. 1990, AAVSO, private communication  
 Mayall, M. W. 1965, *PASC*, 59, 245  
 Morris, M. 1987, *PASP*, 99, 1115  
 ———. 1990, in *From Miras to Planetary Nebulae: Which Path for Stellar Evolution?* ed. M. O. Mennessier & A. Omont (Montpellier: Editions Frontières) 520  
 Morris, M., & Barnbaum, C. 1993, in *IAU Symp. 155, Planetary Nebulae* ed. R. Weinberger & A. Acker (Dordrecht: Kluwer), 349  
 Mufson, S. L., & Liszt, H. S. 1975, *ApJ*, 202, 183  
 Najita, J. 1993, Ph.D. thesis, Univ. California, Berkeley  
 Parsons, S. B. 1971, *ApJ*, 164, 355  
 Pascoli, G. 1987, *A&A*, 180, 191  
 Phillips, J. G., & Freedman, R. S. 1969, *PASP*, 81, 521  
 Phillips, J. P., & Reay, N. K. 1977, *A&A*, 59, 91  
 Reid, M. J., & Dickinson, D. F. 1976, *ApJ*, 209, 505  
 Romanik, C. J., & Leung, C. M. 1981, *ApJ*, 246, 935  
 Sahai, R., & Wannier, P. G. 1988, *A&A*, 201, L9  
 Shu, F. H., Lizano, S., Ruden, S. P., & Najita, J. 1988, *ApJ*, 328, L19  
 Shu, F. H., Najita, J., Ostriker, E., Wilkin, F., Ruden, S., & Lizano, S. 1994, *ApJ*, 429, 781  
 Soderblom, D. R., Pendelton, J., & Pallavicini, R. 1989, *AJ*, 97, 539  
 Soker, N. 1992, *ApJ*, 389, 628  
 ———. 1993, in *Mass Loss on the AGB and Beyond*, ed. H. Schwarz (CTIO/ESO Workshop, Chile) (Munich: ESO) 18  
 Soker, N., & Livio, M. 1989, *ApJ*, 339, 268  
 Tassoul, J. L. 1978, *Theory of Rotating Stars* (Princeton: Princeton Univ. Press)  
 Tonry, J., & Davis, M. 1979, *AJ*, 84, 1511  
 Tsuji, T., Unnow, W., Kaifu, N., Izumiura, H., Ukita, N., Cho, S., & Koyama, K. 1988, *ApJ*, 327, L23  
 Vogt, S. S. 1987, *PASP*, 99, 1214  
 Zuckerman, B., & Aller, L. W. 1986, *ApJ*, 301, 772